Iranian Journal of Medical Physics

ijmp.mums.ac.ir

Characterization of the Radioluminescence Response of Ge-Doped Silica Fibers for 6 MV Radiotherapy Beam Profile Dosimetry

Md Masud Alam[1], Rajada Khatun[2*], Mir Tahsin Ahmed[3], Md. Abul Hasnat[4], H.T. Zubair[5], Shirin Akter[2], Ashrafun Nahar Monika[2], Md. Kabir Uddin Sikder[1]

1. Department of Physics, Jahangirnagar University, Savar, Dhaka, Bangladesh
2. Medical Physics Division, Atomic Energy Centre, Dhaka, Bangladesh
3. Department of Nuclear Engineering, University of Dhaka, Dhaka, Bangladesh
4. Institute of Nuclear Medical Physics, AERE, Savar, BAEC, Bangladesh
5. Center for Fiber Networking and Communication, COE for Intelligent Network, Multimedia University, 63100 Cyberjaya, Selangor, Malaysia

ARTICLE INFO

Article type:
Original Paper

Article history:
Received: Apr 13, 2025
Accepted: Sep 29, 2025

Keywords:
In-Vivo Dosimetry
Radioluminescence
Ge-Doped Silica Fiber
Beam Profile
Flatness
LINAC

ABSTRACT

Introduction: Accurate radiation dose measurement in both target and non-target tissues is essential in modern external beam radiotherapy. In dosimetry systems, the goal is to deliver the maximum dose to the target volume while ensuring minimal exposure to the surrounding normal cells. Among various medical dosimetry systems like thermoluminescence (TL), optically stimulated luminescence (OSL), and radioluminescence (RL), the RL system offers a real-time monitoring system.

Material and Methods: This study aims to characterize the Ge-doped probe in making beam profile measurements using the myDoz® RL/OSL dosimetry system and comparing its accuracy with a CC-13 ion chamber. The RL system utilized a 30-meter PMMA optical fiber with a Ge-doped optical fiber scintillator probe. Beam profiles were measured for 3 × 3 and 10 × 10 cm² field sizes at a depth of 1.5 cm in solid water, with a source-to-surface distance (SSD) of 100 cm, using a 6 MV photon beam, 400 MU/min dose rate, and a total dose of 3 Gy.

Results: The RL readout mechanism enabled instantaneous dose and dose-rate readings. The results showed high consistency and close agreement with the CC-13 ion chamber, with beam profiles displaying uniform central dose, sharp penumbra, and strong symmetry. Larger fields exhibited increased flatness due to photon dispersion. Moreover, the dose distribution out-of-field may still cause low-dose exposure to normal tissues.

Conclusion: To sum up, Ge-doped fibers demonstrated excellent real-time, high-resolution performance, making them promising alternatives to traditional dosimeters. Future research should focus on clinical implementation and system optimization for advanced radiotherapy methods.

► *Please cite this article as:*
Alam MM, Khatun R, Ahmed MT, Hasnat MA, Zubair HT, Akter Sh, Monika AN, Md. Sikder KU. Characterization of the Radioluminescence Response of Ge-Doped Silica Fibers for 6 MV Radiotherapy Beam Profile Dosimetry. Iran J Med Phys 2025; 22: 209-217. 10.22038/ijmp.2025.87703.2538.

Introduction

Radiotherapy is the use of ionizing radiation to treat cancer, and in Bangladesh, radiation therapy is used to treat more than 60% of all cancer patients [1]. The effectiveness of radiotherapy depends on the ability to accurately predict and measure the radiation dose received by the entire irradiated volume. Consequently, there is a demand for new, in vivo radiation monitoring systems capable of real-time body dose measurement, facilitating the precise delivery of radiation to tumor cells by linear accelerators while sparing adjacent healthy tissues [2].

Several types of devices (dosimeters) have been explored to characterize absolute dose in radiation therapy, including thermoluminescence dosimeters (TLDs), optically stimulated luminescence dosimeters (OSLDs), radioluminescence dosimeters (RLDs), silicon diodes, radiochromic films, metal-oxide-semiconductor field-effect transistors (MOSFETs), and ionization chambers (ICs) [3-6]. In radiation dosimetry, researchers focus on developing dosimetric sensors for real-time dose measurements. To mitigate these challenges, different techniques are used for radiation sensing, including TL, which is incapable of providing real-time measurements, as its operation depends on heat [7]. Techniques employing light as the stimulating source have demonstrated more accuracy, feasibility, and efficiency compared to heat-based methods, particularly when real-time measurement is considered. Over the past two decades, OSL has emerged as a prominent dosimetry

*Corresponding Author: Tel: +88-01552643272; Fax: 88-02-58617946; Email: rajadakhatunhasi@gmail.com

technique, with commercialization by leading dosimetry service providers [8]. The advantages of the OSL technique include its high sensitivity, efficient light delivery via optical waveguides, rapid readout times, and the use of relatively simple reader equipment, which is characterized by the emission of light from an irradiated material when stimulated by light. A predecessor phenomenon is known as radioluminescence (RL) [9] refers to the prompt emission of light from a dosimetric material upon exposure to ionizing radiation. It arises from the recombination of electrons and holes at specific recombination centers, typically emitting light at wavelengths like fluorescence. The holes move toward the top of the valence band while the electron moves toward the bottom of the conduction band when exposed to radiation. This configuration allows the electron-hole pairs to recombine in a variety of ways. Due to its spontaneous nature, RL is predominantly utilized to monitor dose rates. Over the last thirty years, extensive research has been conducted on RL, which results from ionizing radiation interacting with optically transparent materials. This suggests that RL is a promising option for radiation dosimetry in a real-time dosimetry system. While RL research on real-time medical dosimetry is still in its early stages, there is growing interest in this field as real-time radiation dose measurement becomes more prevalent [5, 9-11].

Since doped silica optical fibers offer the distinct potential and promise of remote monitoring at comparatively great distances from the radiation source, they demonstrate promising RL properties for quick evaluation and real-time dosimetry [5-6]. The luminescence properties of Ge-doped SiO_2 are significantly influenced by the dopant concentration within the fiber core [12]. Additionally, the signal from a Ge-doped silica optical fiber has been utilized to investigate phenomena such as memory effects, afterglow, and the plateau behavior of RL under photon beam irradiation from a medical linear accelerator (LINAC). This study demonstrates the potential of intentionally fabricated Ge-doped optical fibers as radiation sensors, leveraging RL technology to enable rapid readout of absorbed radiation and facilitate real-time, remote monitoring of dose rates to obtain the RL response to LINAC irradiations. A prototype photomultiplier tube (PMT) based reader system is employed to record the responses from the RL [5, 9]. Recently, an RL dosimetry system with germanium-doped optical fiber provided suitable real-time data and was found to be free from spectral superposition or noise, also exhibiting energy independence in the use of X-rays generated at 6 and 10 MV [9, 12].

Based on the above literature discussions, we establish a method for the characterization of the Ge-doped silica fiber probe in making beam profile measurements using typically available clinical physics equipment, whereas we use Ge-doped silica fiber to verify how accurately it measures real-time radiation dose during treatment. Compared to a standard ion chamber, it showed precise and reliable dose measurements for both small and large fields. Its small size and fast response make it valuable for real-time patient dose monitoring. This validation of real-time dosimetry accuracy is the key novelty of our work. This method is then followed to produce an available dataset of the beam profile dose distribution of our clinical LINAC using the myDoz®RL/OSL dosimetry system.

Materials and Methods

Medical Linear Accelerator

The medical LINAC was the primary apparatus used in external beam radiation therapy treatments. With the use of the LINAC, a patient's tumor can be precisely targeted with high-energy photons (also known as x-rays) or electron beams to eradicate cancer cells while safeguarding nearby healthy tissues. For this study, we employed a Varian LINAC-ix at INMP, AERE, Dhaka, Bangladesh, for investigation.

myDoz®RL/OSL Dosimetry System

The Hamamatsu Photon Counting Head H7421 [13] series was employed for RL signal counting, leveraging its exceptional sensitivity for detecting and quantifying low light levels. These PMTs are a critical component in scientific, medical, and industrial applications requiring precise low-light detection. Its broad spectral range, spanning from ultraviolet to near-infrared wavelengths, combined with rapid response times and high sensitivity, ensures accurate signal measurement.

Ge-Doped SiO_2 Glass Fiber

For dosimetric applications, the germanium (Ge) dopant within the SiO_2 core plays a pivotal role in the RL dosimetry system. Optical fibers, typically designed as waveguides for telecommunication, are commercially available with minimal Ge doping levels to meet their intended use. However, such low concentrations may not suffice to generate the defect centers necessary for reliable dosimetric performance. Therefore, the fabrication of SiO_2:Ge fibers with controlled and well-defined Ge compositions was essential for this study. The SiO_2:Ge optical fibers used in this study as dosimeter materials were fabricated using the Modified Chemical Vapor Deposition (MCVD) technique, leveraging the facilities at the Multimedia University MCVD Laboratory. The MCVD process involved sequential steps, starting with tube cleaning (using Suprasil F-300 synthetic quartz glass) and high-temperature fire polishing (1600 - 2000 °C). This was followed by the chemical oxidation reaction of $SiCl_4$, $GeCl_4$, and O_2 to produce SiO_2 and GeO_2 at approximately 1300 °C, leading to the deposition of oxide particles (SiO_2, referred to as soot, and GeO_2). The deposited particles were then consolidated at 1500 - 1800 °C, and the tube collapsed at 1900 - 2100 °C to form the preform. The preform was subsequently drawn

into fibers with dimensions of 604/100 µm (total diameter/core diameter) using the fiber-pulling tower at the University of Malaya. The fibers were then cut with high precision using a Fujikura CT-30 cleaver, mounted on stainless steel holders with carbon tape, and analyzed for quality assurance using SEM–EDX techniques under a 30 kV electron beam [14].

Probe Preparation

Probes incorporating RL sensors were fabricated using 1.9 cm long 100 µm core silica optical fiber, which is represented in Figure 1 a. This segment was coupled to 30 m lengths of SH4001 Super ESKA polymethyl methacrylate (PMMA) optical fiber, featuring a typical 1 mm core diameter. Precise alignment of the SiO_2:Ge fiber core with the PMMA fiber core was achieved to optimize signal transmission. A lightproof coating was applied to the assembly using an opaque black tape for effective shielding, which is represented in Figure 1 b.

Irradiation Setup

The RL response was evaluated under 6 MV photon beams generated by a medical LINAC (Varian LINAC-ix). The source-to-surface distance (SSD) was maintained at 100 cm, with an irradiation field size of 3×3 cm^2 and 10×10 cm^2 (Figure 2). The probe head was positioned at the maximum dose point (D_{max}) of 1.5 cm below the surface for 6 MV photon beam at 400 MU/ min and a dose of 3 Gy with 0° gantry angle, within a solid water phantom. During irradiation, the emitted RL signal was transmitted via a 30 m-long PMMA fiber through a radiation-shielded thick wall to the acquisition terminal located outside the radiation chamber and linked to a reader that was installed in the control room.

To obtain the RL signal, the LED source was left off for myDoz®RL/OSL dosimetry system, and a convex lens was used to direct the light onto a dichroic beam splitter. The RL signal was divided and reflected by the beam splitter. It was then retransmitted through the PMMA fiber and directed to a PMT (300 − 700 nm) via a bandpass filter (315 − 445 nm). In signal processing, a photon counting unit was connected to a workstation and a PMT by acting as a bridge. The procedure for gathering data was managed via a Labview interface from National Instruments. To get the RL signal for a gate time of 500 ms, the myDoz®RL/OSL dosimetry system automatically settled for the maximum possible measurement number of 100000 and a measurement time of 50000 seconds, but the signal data count completed within 2000 seconds. These parameters were selected to ensure precise control of the PMT during the experiment, facilitating accurate real-time RL dosimetry. Finally, the experimental data were systematically stored in a TAB file format using Microsoft Excel to facilitate subsequent analysis. Using the normalized RL (%) and ion-chamber (%) values at each lateral position, mean difference (bias), standard deviation (σ) of difference, correlation coefficient (r), and paired t-test for mean difference were calculated to evaluate whether RL can be a candidate for such a measurement over the ion chamber or not.

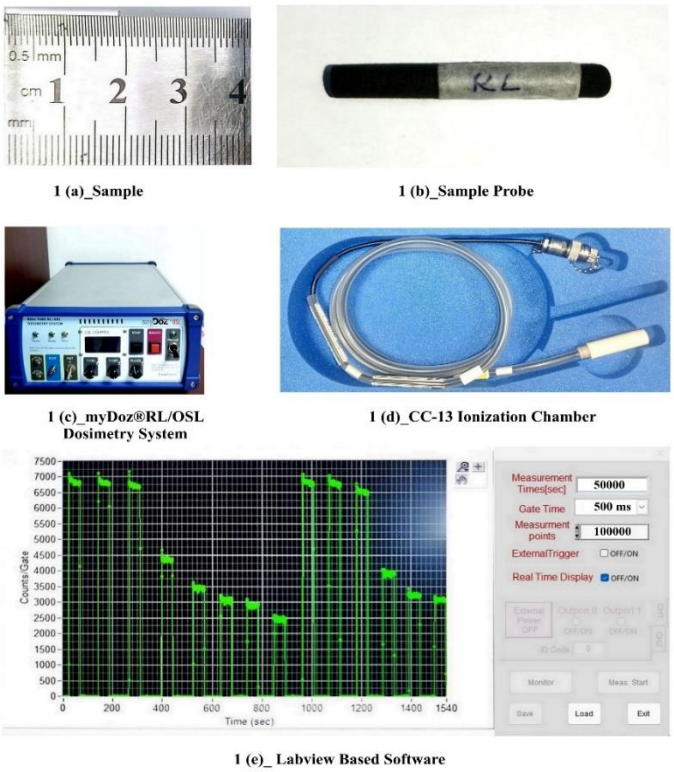

Figure 1. Graphical represents a) the sample of Ge optical fiber, b) sample probe, c) myDoz®RL/OSL Dosimetry System for RL signal measurements, d) CC-13 ion chamber for dose measurements, e) Labview based software interface for data acquisition.

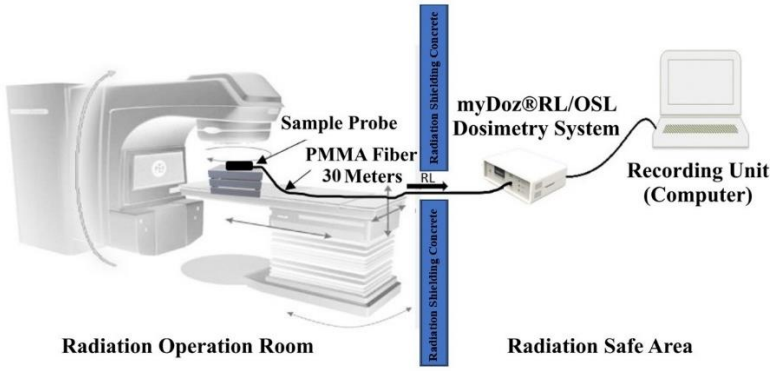

Figure 2. Schematic diagram of the experimental setup for RL dosimetry at 3 × 3 and 10 × 10 cm^2 beam profiles.

Results

Two PMMA fiber-optic cables, one with the Ge-doped fiber sample and another without, were irradiated under identical conditions. The background signal, comprising stem effects (Cerenkov radiation and fluorescence) and inherent RL from the PMMA fiber, was measured using the bare PMMA fiber cable. This background was subsequently subtracted from the total photon counts recorded using the Ge-doped dosimeter sample, which included RL contributions from both the dosimeter and the PMMA fiber, to isolate the dosimeter-specific RL signal [12, 15-17]. The resultant RL yields were then used in evaluating the dose rate, linearity of response to dose, energy dependence, PDD, and characterization of the Ge-doped probe in making beam profile measurements [12].

For 6 MV X-ray irradiations, dose-rate levels exhibit minimal initial fluctuations before rapidly stabilizing [12]. Fluctuations in radiation output intensity were a characteristic feature of most LINACs, arising from beam stabilization dynamics and pulse-to-pulse variations. These dose-rate variations were particularly evident during the initiation phase of exposure, typically stabilizing within a few seconds. Despite these transient fluctuations, the output remained within the tolerances specified by manufacturers and did not impact the total dose delivered during radiotherapy [18]. The beam profiles for 3 × 3 cm^2 and 10 × 10 cm^2 were obtained for photon energies of 6 MV, and the beam profiles are displayed in Figures 3 and 4.

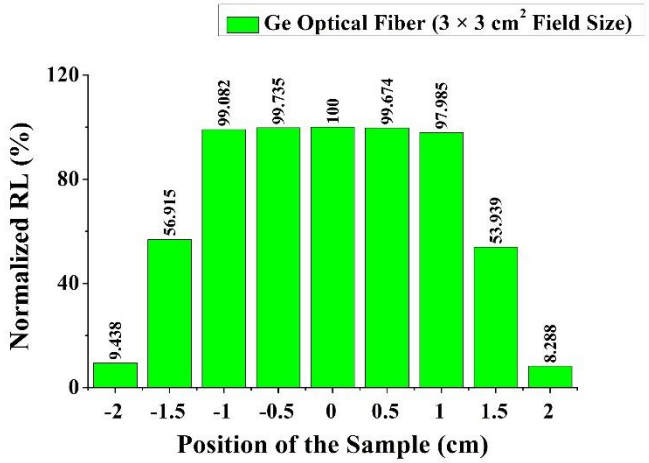

Figure 3. Transverse beam profile of a 3 × 3 cm² small field using Ge optical fiber, whereas the position of the sample range spans from −2.0 cm to +2.0 cm, and nine times repetition of measurement in different positions.

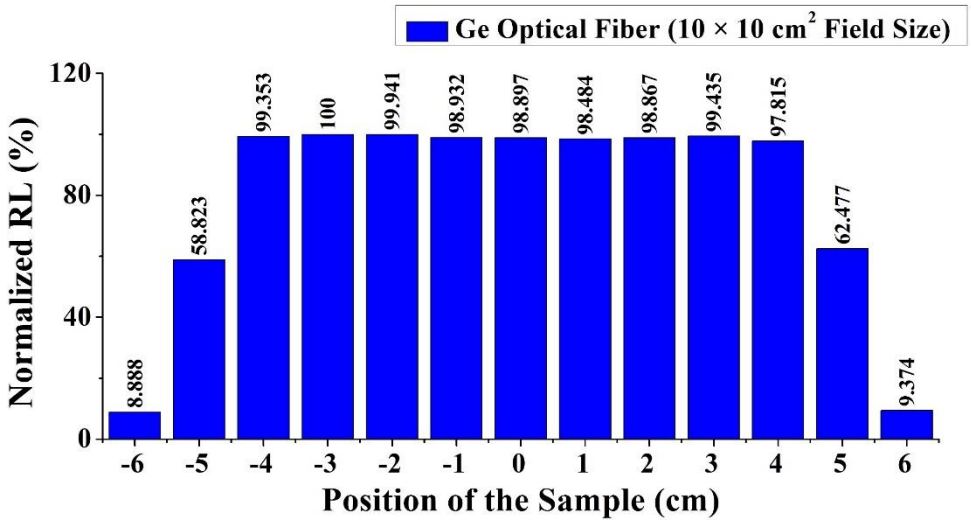

Figure 4. Transverse beam profile of a 10 × 10 cm² field using Ge optical fiber, whereas the position of the sample range spans from −6.0 cm to +6.0 cm, and thirteen times repetition of measurement in different positions.

Positional Response Characteristics of the RL Detector in a 3 × 3 cm² Photon Field

To investigate the variation in RL signal and normalized RL due to different positions in a 3 × 3 cm², its parameters were fixed, like field size, SSD, depth, dose rate, photon energy, and dose. It had been followed that the ideal shift should align with the symmetry of the cross-beam profile, and the ideal shifts should be 0.5 cm negative and 0.5 cm positive from the center to a maximum of 2 cm on both sides of the beam profile. The data were stored in Excel for analysis. To get normalized data, the RL signal of the position of the sample was divided by the maximum RL signal and multiplied by 100 to get Normalized RL, which indicates the dose distribution per percentage in the beam profile. The RL signal and normalized RL are computed in Table 1.

From Table 1, it has been observed that the RL and normalized RL demonstrated a clear peak at the center of the beam, where the maximum RL (492674 counts/s) corresponded to 100% of the normalized RL. The profile has exhibited symmetry at the center, with positions equidistant from the center showing comparable RL values. The position of the negative and the positive on both sides has been denoted as the dose distribution inside and outside of the field that subjectifies the position at the center. For instance, at both 1 cm negative and 1 cm positive, the normalized RL values are 99.082% and 97.985%, respectively, reflecting a well-aligned beam profile. Besides, at the edges by both 1.5 cm negative and positive from the center of the field size, the normalized RL values are decreased to 56.915% and 53.939%, respectively, which signifies dose distribution suddenly reduces, and the results are remarkable. The position of the probe from both 2 cm of negative and positive sides is located near the field size, which is denoted as the outside of the field position. A graphical representation has been depicted in Figure 3 for better acknowledgment of the 3 × 3 cm² beam profile. The dose distribution of the outside field is not eliminated, which can be clearly visualized in Figures 3 and 4.

Positional Response Characteristics of the RL Detector in a 10 × 10 cm² Photon Field

In radiotherapy, real-time RL dosimetry is feasible when readings are highly reproducible, linear with absolute dose, and consistent with dose rate. Moreover, with the fiber-coupled RL dosimeter, the measured dose should exclude any spurious contributions from the signal carrier, specifically stem signals generated in the PMMA fiber, to enable accurate determination of the absolute dose [12]. A PMT-based RL reader was constructed to evaluate the contribution of Ge-doped silica optical fiber to the RL signal during irradiation by photon beams from a clinical linear accelerator. Therefore, the Ge-doped RL dosimetry system demonstrates a distinct capability for true real-time dose-rate monitoring, providing immediate feedback to the operator.

To measure the RL and normalized RL across different positions in a 10×10 cm² field, it was followed that the ideal shift should align with the symmetry of the cross-beam profile, and the ideal shifts should be both 1 cm negative and 1 cm positive from the central axis to a maximum of 6 cm on both sides of the field. The normalized RL signal process is described in a 3 × 3 cm² beam profile. The data were stored in Excel to analyze, and the RL and normalized RL are computed in Table1 & 2. The tabulated data represent the Position of the sample in cm, Depth in cm, SSD in cm, Monitor unit, Energy in MV, Couch shift increment in cm, RL in counts/s, Normalized RL in percentage, Ion Chamber in percentage, and dose distribution for Ge optical fiber at a 10 × 10 cm² beam profile across lateral positions from the central axis.

The normalized RL profile for the 10 × 10 cm² beam exhibits excellent uniformity within the central

region (–4 cm to +4 cm), confirming the stability and flatness of the radiation field essential for accurate dose delivery. Beyond this range, the RL response declines sharply, delineating the penumbra and out-of-field regions where the photon fluence decreases rapidly. This pronounced fall-off reflects the expected characteristics of a well-collimated photon beam and demonstrates the detector's capability to accurately capture spatial dose variations across the field.

Comparison of Normalized RL and Ion Chamber Dosimetry at a 3 × 3 cm² Beam Profile

Dosimetric measurements were conducted in a clinical radiotherapy environment using a LINAC model to evaluate the beam profiles of the RL and CC-13 ion chamber, which are represented in Figure 5. The measurements were performed symmetrically on both the negative and positive sides of the beam profile, and the normalized RL was compared with that of a CC-13 ion chamber to ensure the accuracy and reliability of this experiment. For the 3 × 3 cm^2 beam profile, the calculated mean difference between the RL and the CC-13 ion chamber is -3.32%, with a standard deviation of 7.73%. A strong linear correlation is observed between the two methods ($r \approx 0.98$). The paired t-test ($n = 9$, $t \approx -1.29$, critical $t_{0.05} = 2.306$, $df = 8$) indicated that $|t| < t_{0.05}$, confirming the difference between the RL and the CC-13 ion-chamber responses is not statistically significant. In comparison, the RL and ion-chamber measurements are statistically similar ($p > 0.05$) and exhibit only minor deviations in the penumbra region due to a sharp decline in dose distribution. Therefore, the RL has demonstrated strong agreement with the ion chamber within the beam profile, confirming its reliability for in-field measurements. For small field sizes, the beam flatness reaches a minimum, and the dose distribution at the field center exhibits the maximum dose compared to other in-field positions [19]. This observation, measured at a depth of 1.5 cm for a 6 MV photon beam, confirms the characteristic profile of a small field size displayed in our study [19].

Comparison of Normalized RL and Ion Chamber Dosimetry at a 10 × 10 cm² Beam Profile

The dose distribution for a 10 × 10 cm^2 radiation field was analyzed by comparing normalized RL and CC-13 ion chamber measurements at a depth of 1.5 cm for a 6 MV photon beam, which is represented in Figure 6. For the beam profile, the mean difference (Δ) between the RL and the CC-13 ion chamber is -4.25%, with a standard deviation of 8.79%. A strong correlation is observed between the RL and CC-13 ion-chamber measurements ($r \approx 0.97$). The paired t-test ($n = 13$, $t \approx -1.74$, critical $t_{0.05} = 2.179$, $df = 12$) indicated that $|t| < t_{0.05}$, representing no statistically significant difference ($p > 0.05$) between the RL and the CC-13 ion-chamber. The minimum deviation in the penumbra region and high correlation confirm excellent agreement between the dose profiles obtained from RL and the CC-13 ion chamber. This agreement indicates uniform dose deposition across the field's central region, confirming the beam's stability and the reliability of both measurement methods for characterizing dose uniformity. Besides, at the edges, slight differences are observed between the RL and CC-13 ion chamber measurements, where the ion chamber measurements drop more sharply. Therefore, both normalized RL and ion chamber confirm the alignment and consistency of the 10 × 10 cm² beam profile. The close agreement between the two measurement methods further validates the suitability of Ge optical fiber detectors for precise dosimetry.

Moreover, beam flatness has increased with increasing field size due to the enhanced dispersion of photon beams as the field size expands. We notice that for the 10 × 10 cm² beam profile, the dose change is obtained at a certain depth along the vertical line to the central axis at a depth of 1.5 cm for a 6 MV photon energy, that expected for the beam profile of a LINAC [19].

Table 1. The tabulated data represents the position of the sample in cm, Depth in cm, SSD in cm, Monitor unit, Energy in MV, Couch shift increment in cm, RL in Counts/s, Normalized RL in percentage, Ion Chamber in percentage, dose distribution for Ge optical fiber at 3 × 3 cm² small size beam profile across lateral positions from the central axis.

Position of the sample (cm)	Depth (cm)	SSD (cm)	MU	Energy (MV)	Couch shift increment (cm)	RL (Counts/s)	Normalized RL (%)	Ion Chamber (%)
− 2.0	1.5	100	300	6	0.5	46498	9.438	9.75
− 1.5	1.5	100	300	6	0.5	280403	56.915	70.45
− 1.0	1.5	100	300	6	0.5	488151	99.082	96.28
− 0.5	1.5	100	300	6	0.5	491368	99.735	99.60
0	1.5	100	300	6	0.5	492674	100.000	99.40
+ 0.5	1.5	100	300	6	0.5	491068	99.674	98.86
+ 1.0	1.5	100	300	6	0.5	482745	97.985	97.87
+ 1.5	1.5	100	300	6	0.5	265741	53.939	73.53
+ 2.0	1.5	100	300	6	0.5	40835	8.288	9.20

Table 2. The tabulated data represent the position of the sample in cm, Depth in cm, SSD in cm, Monitor unit, Energy in MV, Couch shift increment in cm, RL in Counts/s, Normalized RL in percentage, Ion Chamber in percentage, dose distribution for Ge optical fiber at 10 × 10 cm² beam profile across lateral positions from the central axis.

Position of sample (cm)	Depth (cm)	SSD (cm)	MU	Energy (MV)	Couch shift increment (cm)	RL (Counts/s)	Normalized RL (%)	Ion Chamber (%)
− 6	1.5	100	300	6	1	31852	8.888	15.76
− 5	1.5	100	300	6	1	210800	58.823	83.44
− 4	1.5	100	300	6	1	356047	99.353	97.07
− 3	1.5	100	300	6	1	358366	100.000	98.88
− 2	1.5	100	300	6	1	358153	99.941	99.78
− 1	1.5	100	300	6	1	354538	98.932	99.76
0	1.5	100	300	6	1	354412	98.897	99.58
+ 1	1.5	100	300	6	1	352933	98.484	99.44
+ 2	1.5	100	300	6	1	354304	98.867	99.36
+ 3	1.5	100	300	6	1	356340	99.435	98.53
+ 4	1.5	100	300	6	1	350536	97.815	95.74
+ 5	1.5	100	300	6	1	223897	62.477	83.94
+ 6	1.5	100	300	6	1	33593	9.374	15.24

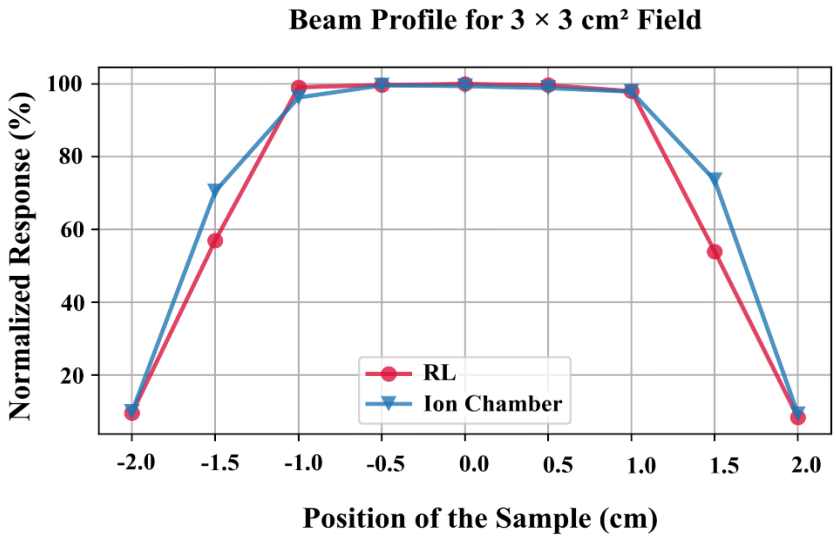

Figure 5. Comparison of the transverse profile obtained on a 3 × 3 cm² 6 MV photon beam using Ge optical fiber and CC-13 ion chamber, whereas the position of the sample range spans from −2.0 cm to +2.0 cm, and nine times repetition of measurement in different positions.

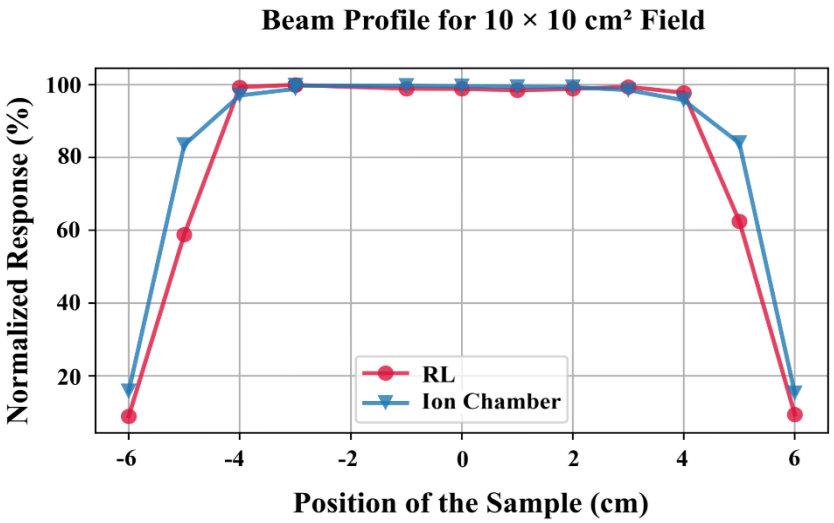

Figure 6. Comparison of the transverse profile obtained on a 10 × 10 cm² 6 MV photon beam using Ge optical fiber and CC-13 ion chamber, whereas the position of the sample range spans from −6.0 cm to +6.0 cm, and thirteen times repetition of measurement in different positions.

Discussion

In radiotherapy, the treatment table is called the couch, and a couch shift means moving the table to align the patient. Whereas the treatment couch position represents a crucial clinical parameter to prevent gross setup errors. However, the position captured at the initial treatment setup becomes erroneous during data reporting when the couch shifts are incorrectly specified in the treatment plan or improperly applied during patient setup [20].

The RL dosimetry system, particularly using Ge-doped optical fiber, demonstrated its capacity for providing real-time dose measurements in clinical settings. The results from both the 3 × 3 and 10 × 10 cm² beam profiles reveal that RL measurements offer reliable and reproducible dose distributions across different positions in the beam profile.

The RL and normalized RL analyses demonstrated a symmetrical and precisely aligned dose distribution within the 3 × 3 cm² beam profile, exhibiting peak intensity at the center of the beam profile and significant dose gradients toward the field edges. Notably, out-of-field dose distributions, despite their reduced intensity, can result in low-dose radiation exposure to adjacent normal tissues, potentially contributing to unintended biological effects, emphasizing the importance of precise beam characterization in radiation treatment planning.

The 10 × 10 cm² beam profile demonstrated highly symmetrical and consistent normalized RL responses within the central ±4 cm region, confirming the Ge-doped fiber's precision and reproducibility in dose measurement. The sharp fall-off at the edges of the field reinforces the importance of precise dose control in clinical radiotherapy, especially in protecting adjacent normal tissues. So, the Ge optical fiber detector has provided accurate, reliable, and reproducible dose measurements, validated by the symmetry and consistency of the RL data.

The comparison of RL measurements with CC-13 ion chamber dosimetry further validates the reliability of the RL system. Both beam profiles exhibit strong agreement in the central region of the beam, indicating that RL dosimetry is a reliable tool for dose measurements in clinical settings. The slight differences observed at the field edges can be attributed to the inherent differences in the measurement principles of the two methods, but it does not detract from the overall consistency and accuracy of the RL system.

In our study, for both small and large fields, we observed that penetrating power decreases with increasing depth. Furthermore, beam flatness increases with increasing field size because the photon beam dispersion increases with increasing field size. This is due to the increased obliquity of the photon beam at the edges of the blocks at collimator openings increases with field size, which agrees with the results reported in both literatures [19, 21].

A key limitation of this study on LINAC beam profile characterization using RL dosimetry is the stem effect, which interferes with real-time RL signal accuracy. Although Ge-doped silica glass exhibits some OSL properties, its contribution is minimal compared to the RL response, limiting its practical use. Future work should focus on minimizing the stem effect during radiotherapy to improve measurement reliability. This can be achieved by developing mathematical models to correct for environmental influences and by establishing standardized OSL protocols to enhance dosimetric accuracy. These improvements will help optimize the RL dosimetry system for more precise and reliable beam profile assessments in clinical settings.

Conclusion

The experimental characterization of the Ge-doped optical fiber probe for beam profile measurements demonstrated consistent, reliable, and reproducible dose data closely aligned with CC-13 ion chamber measurements. Additionally, for the 3 × 3 cm² and 10 × 10 cm² beam profiles, the RL measurements captured uniform dose distribution within the central beam region and steep dose fall-offs at the penumbra, aligning with the expected characteristics of well-collimated photon beams. The high symmetry in the RL profiles validated precise beam alignment and dosimetric accuracy. Besides, out-of-field dose distribution may still cause low-dose exposure to normal tissues. Moreover, the increase in beam flatness with larger field sizes was clearly observed due to photon beam dispersion. Overall, these results confirm the suitability of Ge-doped fibers as real-time, high-resolution dosimeters and highlight their potential as effective alternatives to conventional dosimetry tools. This technology promises to enhance radiotherapy dosimetry through improved calibration, monitoring, and quality assurance of the LINAC. Future research should explore broader clinical applications and further optimization of the RL dosimetry system for advanced cancer treatment modalities.

Acknowledgment

We thank the faculty and staff of the Department of Radiation Oncology of the Institute of Nuclear Medical Physics (INMP) for the cooperation extended to this study.

References

1. Rahman S. Organ risk assessment by TLO to improve treatment planning of cancer patients in Bangladesh. 2003.
2. Zhuang Q, Li J, Li Y, Zhu S, Liu Y, Wang Z. Embedded structure fiber-optic radiation dosimeter for radiotherapy applications. Opt Express. 2016;24(5):5172–85.
3. Lambert J, Nakano T, Law S, Elsey J, McKenzie DR, Suchowerska N. In vivo dosimeters for HDR brachytherapy: a comparison of a diamond detector, MOSFET, TLD, and scintillation detector. Med Phys. 2007;34(5):1759–65.

4. Hyer DE, Fisher RF, Hintenlang DE. Characterization of a water-equivalent fiber-optic coupled dosimeter for use in diagnostic radiology. Med Phys. 2009;36(5):1711–6.
5. Rahman AKMM, Rahman M, Uddin M, Zubair HT, Khan SR, Ahmed F, et al. Radioluminescence of Ge-doped silica optical fibre and Al2O3:C dosimeters. Sens Actuators A Phys. 2018;270:72–8.
6. Benevides LA, Huston AL, Justus BL, Falkenstein P, Brateman LF, Hintenlang DE. Characterization of a fiber-optic-coupled radioluminescent detector for application in the mammography energy range. Med Phys. 2007;34(6):2220–7.
7. McKeever SWS, Moscovitch M. Topics under debate: On the advantages and disadvantages of optically stimulated luminescence dosimetry and thermoluminescence dosimetry. Radiat Prot Dosimetry. 2003;104(3):263–70.
8. Yukihara EG, McKeever SWS, Akselrod MS. State of art: Optically stimulated luminescence dosimetry – frontiers of future research. Radiat Meas. 2014;71:15–24.
9. Rahman AKMM, Rahman M, Uddin M, Khan SR, Ahmed F, Zubair HT, et al. Germanium-doped optical fiber for real-time radiation dosimetry. Radiat Phys Chem. 2015;116:170–5.
10. Zubair HT, Rahman AKMM, Uddin M, Ahmed F, Khan SR, Rahman M, et al. Recent advances in silica glass optical fiber for dosimetry applications. IEEE Photonics J. 2020;12(3):1–25.
11. Molina P, Sommer M, Kattner F, Henniger J. Response characterization of an Y2O3:Eu-based radioluminescence probe under 60Co irradiation. Radiat Meas. 2013;56:338–41.
12. Rahman AKMM, Zubair HT, Uddin M, Ahmed F, Khan SR, Rahman M, et al. Ge-doped silica optical fibres as RL/OSL dosimeters for radiotherapy dosimetry. Sens Actuators A Phys. 2017;264:30–9.
13. Alldatasheet. Product variations specifications metal package PMT with cooler photon counting head H7421 series cooling specifications dark count. [Internet]. [cited 2025 Nov 17]. Available from: https://www.alldatasheet.com
14. Sarhan HG, Zubair HT, Rahman AKMM, Ahmed F, Rahman M. Performance of a Ge-doped optical fibre dosimeter for CT real-time measurements. Radiat Phys Chem. 2023;212:111149.
15. Andersen CE. Fiber-coupled luminescence dosimetry in therapeutic and diagnostic radiology. AIP Conf Proc. 2011;1345:100–19.
16. Arnfield MR, Gaballa HE, Zwicker RD, Islam Q, Schmidt-Ullrich R. Radiation-induced light in optical fibers and plastic scintillators: Application to brachytherapy dosimetry. 1996.
17. Marckmann CJ, Aznar MC, Andersen CE, Bøtter-Jensen L. Influence of the stem effect on radioluminescence signals from optical fibre Al2O3:C dosemeters. Radiat Prot Dosimetry. 2006;119(1–4):363–7.
18. Partridge M, Evans PM, Mosleh-Shirazi MA. Linear accelerator output variations and their consequences for megavoltage imaging. Med Phys. 1998;25(8):1443–52.
19. Chowdhury RI, Ahmed R, Rabby F, Akter M, Rahman M. Beam profile characteristics of a Varian linear accelerator across different photon energy levels. 2024.
20. Wang H, Rea A, Rudek B, Chen T, McCarthy A, Barbee D. Automatic couch position calculation using eclipse scripting for external beam radiotherapy. J Appl Clin Med Phys. 2021;22(2):77–84.
21. Roy SK, Islam Q, Ahmed F, Zubair HT, Rahman AKMM. Dosimetric characteristics of 6 MV medical linac at BAEC. Int J Med Phys Clin Eng Radiat Oncol. 2021;10(1):38.